Journal of Nuclear Medicine, published on October 14, 2021 as doi:10.2967/jnumed.121.262398

Head-to-head comparison of ^{68}Ga-PSMA-11 PET/CT and mpMRI with histopathology gold-standard in the detection, intra-prostatic localization and local extension of primary prostate cancer: results from a prospective single-center imaging trial

Ida Sonni[1], Ely R. Felker[2], Andrew T. Lenis[3], Anthony E. Sisk[4], Shadfar Bahri[1,5], Martin Allen-Auerbach [1,5], Wesley R. Armstrong[1], Voraparee Suvannarerg[2,6], Teeravut Tubtawee[2,7], Tristan Grogan[8], David Elashoff[8], Matthias Eiber[1,9], Steven S. Raman[2], Johannes Czernin[1,5,10], Robert E. Reiter[3,5,10*] and Jeremie Calais[1,5,10*]

1. Ahmanson Translational Theranostics Division, Department of Molecular and Medical Pharmacology, David Geffen School of Medicine, University of California Los Angeles, Los Angeles, CA, USA
2. Department of Radiology, David Geffen School of Medicine, University of California, Los Angeles, CA, USA
3. Department of Urology, University of California Los Angeles, Los Angeles, CA, USA
4. Department of Pathology, David Geffen School of Medicine, University of California, Los Angeles, CA, USA
5. Institute of Urologic Oncology, David Geffen School of Medicine, University of California Los Angeles, Los Angeles, CA, USA
6. Department of Radiology, Faculty of Medicine Siriraj Hospital, Mahidol University, Bangkoknoi, Bangkok, Thailand
7. Department of Radiology, Prince of Songkla University, Karnchanavanij road Hat Yai, Thailand
8. Department of Medicine Statistics Core, University of California Los Angeles, Los Angeles, CA, USA
9. Technical University of Munich, Klinikum rechts der Isar, Department of Nuclear Medicine, Germany
10. Jonsson Comprehensive Cancer Center, University of California Los Angeles, Los Angeles, CA, USA

* Joint senior authorship

Correspondence to: Ida Sonni, MD; Ahmanson Translational Theranostics Division, Department of Molecular and Medical Pharmacology, David Geffen School of Medicine; University of California, Los Angeles, Los Angeles, CA, USA 90095-7370

E-mail: isonni@mednet.ucla.edu

Keywords: PSMA PET/CT, prostate cancer, mpMRI, staging, T-staging.

Total Words count: 6208.

ABSTRACT

The role of prostate-specific membrane antigen (PSMA)-targeted PET in comparison to mpMRI in the evaluation of intraprostatic cancer foci is not well defined. The aim of our study was to compare the diagnostic performances of PSMA PET/CT, mpMRI and PSMA PET/CT+mpMRI using 3 independent blinded readers for each modality and with histopathology as gold standard in the detection, intra-prostatic localization and local extension of primary prostate cancer.

Methods: Patients with intermediate- or high-risk prostate cancer who underwent a PSMA PET/CT as part of the prospective trial (NCT03368547) and a mpMRI prior to radical prostatectomy were included. Each imaging modality was interpreted by 3 blinded independent readers unaware of the other modality result. Central majority rule was applied (2:1). Whole-mount pathology was used as the gold-standard. Imaging scans and whole-mount pathology were interpreted using the same standardized approach on a segment- and lesion-level. A "neighboring" approach was used to define imaging/pathology correlation for the detection of individual prostate cancer foci. Accuracy in determining the location, extraprostatic extension (EPE) and seminal vesicle invasion (SVI) of prostate cancer foci was assessed using receiver operating characteristic (ROC) analysis. Inter-reader agreement was calculated using inter-class coefficient (ICC) analysis.

Results: The final analysis included 74 patients (14/74 - 19%) intermediate risk and 60/74 - 81%) high risk). Cancer detection rate (lesion-based analysis) was 85%, 83% and 87 for PSMA PET/CT, mpMRI and PSMA PET/CT+mpMRI, respectively. ΔAUC between PSMA PET/CT+mpMRI and the two imaging modalities alone for delineation of tumor localization (segment-based analysis) was statistically significant ($p<0.001$), but not between PSMA PET/CT and mpMRI ($p=0.093$). mpMRI outperformed PSMA PET/CT in detecting EPE ($p=0.002$) and SVI ($p=0.001$). On a segment-level analysis, ICC analysis showed moderate reliability among PSMA PET/CT and mpMRI readers using a 5-point Likert scale (range: 0.53 to 0.64). In the evaluation of T-staging, poor reliability was found among PSMA PET/CT readers and poor to moderate reliability was found for mpMRI readers.

Conclusions: PSMA PET/CT and mpMRI have similar accuracy in the detection and intra-prostatic localization of prostate cancer foci. mpMRI performs better in identifying EPE and SVI. For the T-staging evaluation of intermediate to high-risk prostate cancer patients, mpMRI should still be considered the imaging modality of reference. Whenever available, PSMA PET/MRI or the co-registration/fusion of PSMA PET/CT and mpMRI (PSMA PET+mpMRI) should be used as it improves tumor extent delineation.

1. Introduction

Prostate cancer is the most common solid organ malignancy in men, accounting for over 190,000 new diagnoses and over 33,000 deaths in 2020 (*1*). Distant extra-pelvic staging of patients with unfavorable intermediate- and high-risk disease with cross sectional imaging and bone scan is recommended to guide initial therapy (*2,3*).

Current methods used to locally stage prostate cancer and identify the precise location of foci of disease rely on the results of systematic or targeted biopsies and multiparametric magnetic resonance imaging (mpMRI). While targeted biopsies have considerably improved the identification of clinically significant prostate cancer and even allowed for the tracking of biopsy cores over time, there is still over 30% chance of missing clinically significant prostate cancer in men with multifocal disease (*4*). Further, in a cohort of men selected as candidates for focal therapy who underwent radical prostatectomy (RP), nearly half had unidentified bilateral disease and would have been inadequately treated (*5*). Therefore, additional and perhaps complementary methods are needed to better characterize and identify clinically significant prostate cancer foci.

Prostate-specific membrane antigen (PSMA) is a transmembrane cell surface protein overexpressed in prostate cancer cells relative to most other tissues (*6*). PSMA PET/CT has been shown in prospective studies to be highly sensitive and specific for the identification of biochemically recurrent disease and to improve the staging of patients with newly diagnosed disease (*7-9*). Previous studies comparing PSMA PET and mpMRI in the local staging of prostate cancer had overall discordant results. While some studies describe superiority of PSMA PET/CT over mpMRI (*10-12*), others show no significant differences (*13,14*).

The goal of the current analysis was to compare the diagnostic performance of PSMA PET/CT, mpMRI and the combination of the two (PSMA PET/CT+mpMRI) in the detection, intra-prostatic localization and local extension of primary prostate cancer with histopathology as the gold standard using 3 blinded independent readers for each modality.

2. Materials and methods

2.1. Study design and patient population

We report here the results of an exploratory endpoint of a prospective trial conducted at the University of California, Los Angeles (NCT03368547). The primary outcome of the trial was to evaluate the diagnostic performance (sensitivity, specificity, positive predictive value, and negative predictive value) of ^{68}Ga-PSMA-11 PET/CT (PSMA PET/CT) for the detection of regional nodal metastases compared with histopathology at radical prostatectomy in patients with intermediate- to high-risk prostate cancer. The results of the primary endpoint analysis were the foundation of a New Drug Application for ^{68}Ga-PSMA-11 (*15*) and will be reported separately.

For the current study, patients with biopsy-proven intermediate- and high-risk prostate cancer by NCCN (*16*) enrolled in the pivotal trial were included in the analysis if they underwent initial staging with both PSMA PET/CT and mpMRI at our institution and subsenquently underwent RP. Patients treated with androgen deprivation therapy were excluded

from the analysis. The study was done under an investigational new drug approval protocol (IND#130649) and was approved by the local institutional review board (IRB#16-001684).

2.2. mpMRI image acquisition

mpMRI were obtained using a 3-T MRI system using a standardized protocol with pelvic external phased-array coils. The mpMRI protocol included conventional multiplanar T2-weighted imaging, DWI, and DCE MRI, as described previously (*17*).

mpMRI were obtained using a 3-T MRI system (Magnetom Trio, Skyra, or Verio system; Siemens Medical Systems, Malvern, Pa) using a standardized protocol with pelvic external phased-array coils. The mpMRI protocol included T2-weighted turbo spin-echo (TSE), DWI, axial unenhanced T1-weighted, and axial 3D fast-field echo DCEMRI sequences. A small-FOV 3D axial TSE T2- weighted sequence was performed using spatial and chemical-shift encoded excitation (SPACE, Siemens Healthcare), as described in detail previously (*17*,*18*).

2.3. PSMA PET/CT image acquisition

PSMA PET/CT images were acquired after intravenous injection of a median of 192.4 MBq of ^{68}Ga-PSMA-11 (IQR: 185 – 203.5) and a median uptake time of 61.5 minutes (IQR: 58 – 67) using a Biograph 64 or mCT PET/CT scanner; Siemens Medical Systems, Malvern, Pa (axial FOV of 22.1 cm). ^{68}Ga-PSMA-11 (Glu-NH-CO-NH-Lys-(Ahx)-[^{68}Ga(HBEDCC)]) was used as the PSMA ligand (*19*) and was obtained from the Biomedical Cyclotron Facility at UCLA. Oral and intravenous CT-contrast was administered unless contraindicated. A 5-mm slice thickness CT scan was used. All PET images acquired from pelvis to vertex were corrected for attenuation, dead time, random events, and scatter. The time per bed position was based on patient weight (*20*).

2.4. Image analysis

For the purpose of this exploratory endpoint analysis, the PSMA PET/CT and mpMRI were read independently by three board-certified nuclear medicine physicians (MAA, SB and IS with 4, 4 and 1 year experience interpreting PSMA PET/CT, i.e. approximately 250 scan/year, and 19, 7 and 7 year experience interpreting oncologic PET/CT, i.e. approximately 1000 scan/year, respectively) and three radiologists (EF, SV and TT, with 5, 5 and 12 years experience with prostate mpMRI, respectively, approximately 1000 scan/year) using OsiriX (*21*) and DynaCAD softwares, respectively.

All readers were aware of biopsy-proven prostate cancer, but blinded to any other demographic, clinical, pathology and imaging information. Readers were blinded to PSMA PET/CT and mpMRI clinical reports and to other readers' findings. A standardized approach was used for imaging interpretation and assess the presence, location and size of prostate cancer foci (lesions) within the prostate. The analysis was conducted on an individual lesion- and segment-level.

2.4.1. Segment-level analysis (prostate cancer localization)

The prostate was divided into 12 segments using orthogonal axial planes in PSMA PET/CT and oblique axial planes in mpMRI: base, midgland and apex defined as the upper, middle and lower third of the prostate, respectively; right/left and anterior/posterior were defined on axial view by a vertical (sagittal plane) and horizontal line (coronal plane) passing by the center of the prostate, respectively (**figure 1**). The 12 segments used in this analysis represented a compromise between the 41 sectors used in the PIRADS score and the sextants used for PSMA PET in previous studies *(12,22)*. All PSMA PET/CT and mpMRI readers assigned each segment a score using a 5-point Likert scale (PSMA score, resembling the PSMA-RADS version 1.0 (*23*,*24*), and PI-RADS score version 2.1 (*25*), respectively) based on the overall likelihood of prostate cancer. Each reader's 5-point scores were further converted into a binary score (1 and 2 = negative for cancer; 3, 4 and 5 = positive for cancer).

2.4.2. *Lesion-level analysis (prostate cancer detection)*

A maximum of three prostate cancer lesions were listed for each patient and described as the index, secondary and tertiary lesion. Each reader recorded lesion size and other parameters (i.e. SUVmax for PSMA PET/CT and DWI PI-RADS score for mpMRI) to aid in the overall interpretation.

2.4.3. T-staging

The presence of bilateral intraprostatic disease, seminal vesicle involvement (SVI – T3b) and extraprostatic extension (EPE – T3a) were assessed visually in a binary manner. (*26*).

2.4.4. Majority rule and central reads

One lead investigator collected the imaging and pathology reads and conducted the final analysis. A central majority rule (2:1) was used to obtain the final reads for PSMA PET/CT and mpMRI. On a segment-level, lesion-level and T-staging-level analysis, a positivity for cancer involvement in the individual segment, lesion or T-level was considered if at least two out of three readers described it as positive for cancer.

PSMA PET/CT + mpMRI

PSMA PET/CT+mpMRI findings were obtained by combining the central majority reads from the two imaging modalities. In case a segment, lesion or T-level finding was described as positive only on one imaging modalitiy (only on PET or mpMRI) as described above, it was automatically considered positive for PSMA PET/CT+mpMRI.

2.5. Histopathology analysis

Whole mount pathology (tissue sections of 5 mm, histologic sections cut at 5 μm) was read by a Genito-Urinary pathologist (AS with 7 years of whole mount experience) blinded to all imaging results using the lesion- and segment-level approach described above. Each lesion was assessed for the presence, location, size of cancer foci and Gleason grades.

Benign prostatic lesions were not considered and excluded from the detection analysis.

2.6 Imaging/ pathology correlation

To define imaging/pathology correspondence on a lesion-level, an adaptation of a previously described approach was used (*27*) (**figure 1**). This "neighboring" approach did not take into account the number of lesions and allowed the location correspondence to involve the immediately adjacent segments. This approach was used to overcome possible interpretation errors due to: misregistration/misalignment deriving from deformation and shrinkage during fixation commonly happening in the phase of whole mount slices preparation (*28*), different orientation used by PSMA PET/CT, mpMRI and whole mount pathology (prostatectomy specimen cross-section) to define the prostate base, midgland and apical regions.

2.7 Statistical analysis

Patient characteristics and study variables were summarized using mean (standard deviation - SD), median (interquartile range - IQR), or frequency (%), as appropriate. The diagnostic performance of PSMA PET/CT, mpMRI and PSMA PET/CT+mpMRI were compared to histopathological analysis on a lesion- and segment-level. Receiver operating characteristics (ROC) curves and area under the ROC curves (AUCs) were obtained with 95% confidence intervals. ΔAUC confidence intervals and p-values were carried out using DeLong's test.

Inter-rater agreement was calculated using inter-class correlation (ICC) using the 'two way random' model, 'absolute agreement' and 'single measure' options. Statistical analyses were performed using IBM SPSSV25 (Armonk, NY) and p-values <0.05 were considered statistically significant.

3. Results

3.1. Patient population

Between January 2017 and November 2019, 398 patients were enrolled in the trial. 74 patients were included in the final analysis of this study (study flowchart in **figure 2**). The mean time between PSMA PET/CT and mpMRI was 43 (39.9) days (range: -31–123 days), PSMA PET/CT and RP was 54.1 (35.9) days (range: 6–180 days), mpMRI and RP was 100.8 (53.4) days (range: 3–288 days). In 44/74 patients (59%) the mpMRI was performed prior to the biopsy, whereas all PSMA PET/CT scans were obtained after confirmation of a positive biopsy. Patient characteristics are summarized in **table 1**.

3.2. Prostate cancer localization (segment-based analysis)

A total of 425/888 segments (48%) were positive for cancer by pathology. PSMA PET/CT, mpMRI and PSMA+mpMRI described cancer (majority reads 2:1) in 310/888 (35%), 314/888 (35%) and 405/888 (46%) segments, respectively. Results of the segment-level analysis and the ROC curves per reader and per imaging modality are shown in **figure 3a and 3b**. A total of 408/888 segments (46%) were described as harboring clinically significant prostate cancer (Gleason score >3+3=6). Results of a sub-analysis including only clinically significant lesions are shown in **Supplementary figure 1**.

The AUCs (sensitivity/specificity) for PSMA PET/CT, mpMRI and PSMA PET/CT+mpMRI were 0.7 (0.84/0.55), 0.73 (0.86/0.59) and 0.77 (0.77/0.71), respectively. ΔAUC between PSMA PET/CT+mpMRI and the two imaging modalities alone was statistically significant ($p<0.001$), but not between PSMA PET/CT and mpMRI ($p=0.093$).

The AUCs using the PSMA and the PI-RADS score for each individual reader 1, 2 and 3 were 0.69, 0.69 and 0.66 and 0.71, 0.72 and 0.71, respectively.

ICC analysis showed moderate reliability (*29*) among PSMA PET/CT and mpMRI readers using the 5-point Likert scales (PSMA PET/CT: reader1/reader2=0.63, reader1/reader3=0.53, reader2/reader3=0.64; mpMRI: reader1/reader2= 0.61, reader1/reader3= 0.55, reader2/reader3=0.55).

3.3. Prostate cancer detection (lesion-based analysis)

Whole mount pathology identified 109 prostate cancer foci (74/32/3 - index/secondary/tertiary lesions). Using the majority reads (2:1), PSMA PET/CT identified 111 lesions (74/33/4 - index/secondary/tertiary lesions) and mpMRI identified 91 (74/16/1 - index/secondary/tertiary lesions). Results of the lesion-level analysis and detection rates for all cancerous lesions are shown in **table 2.** Individual readers' results are shown in **supplementary table 1**.

Detection rate was 85%, 83% and 87% for PSMA PET/CT, mpMRI and PSMA PET/CT+mpMRI, respectively. PSMA PET/CT identified 4 lesions (1 primary and 3 secondary) missed by mpMRI, whereas mpMRI identified 2 lesions (1 primary and 1 secondary) that were missed by PSMA PET/CT (**Supplementary table 2**). Differences in detection rates between PSMA PET/CT and mpMRI were not statistically significant. The addition of PSMA PET/CT did not provide significant increases in detection rates over mpMRI alone.

Two separate sub-analyses excluding small cancerous lesions (≤ 0.5 cm on histopathological analysis) and lesions with Gleason score 3+3=6 were conducted.

Twelve/109 lesions (11%) were graded as Gleason score 3+3=6 (10/12 secondary lesions and 2/12 tertiary lesions). Overall detection rate excluding these lesions was 95% for PSMA PET/CT+mpMRI (vs 92% for both PSMA PET/CT and mpMRI alone).

Detection rates for clinically significant are summarized in **table 2**.

Five/109 lesions (5%) measured ≤ 0.5 cm on histopathological analysis. Three/5 were not detected by either imaging modalities, 1/5 was identified by both and 1/5 was identified by mpMRI and PSMA PET/CT.

Figure 4 and **supplementary figure 2** show examples of PSMA PET/CT, mpMRI and whole mount pathology from our cohort.

3.4. T-staging

Bilateral disease was detected on histopathology in 37/74 patients (50%), SVI in 25/74 (34%) and EPE in 43/74 (58%). By majority reads (2:1), although mpMRI had a higher AUC than PSMA PET/CT for the detection of bilateral disease (0.65 vs 0.54) this was not significantly different (DeLong's test p=0.138) (**figure 3**). mpMRI had a better AUC than

PSMA PET/CT for detection of EPE (0.79 vs 0.59, p=0.002) and SVI (0.84 vs 0.63, p=0.001). The use of PSMA PET/CT+mpMRI did not provide statistically significantly improvements to mpMRI alone.

Poor reliability was found among readers for PSMA PET/CT in the evaluation of bilaterality (ICC= 0.344), EPE (ICC=0.203) and SVI (ICC=0.081); moderately strong reliability was found among mpMRI readers for bilaterality (ICC= 0.693) and EPE (ICC=0.580), poor reliability for SVI (ICC=0.305).

4. Discussion

In our single center study including 74 patients with intermediate- to high-risk prostate cancer, using the majority reads of 3 blinded independent readers for each imaging modality, PSMA PET/CT and mpMRI performed similarly in the detection and intra-prostatic localization of primary prostate cancer, while mpMRI was superior for determining the T-stage. The combined use of PSMA PET/CT and mpMRI improved tumor extent delineation (segment-level analysis) and allowed the identification of multifocal lesions, but did not significantly improve detection rates (lesion-level analysis) of the two modalities alone.

Current clinical guidelines (*2,30*) still recommend the use of cross-sectional imaging (CT or MRI) with bone scan for the extraprostatic distant staging of patients with intermediate- to high- risk prostate cancer. Several studies showed superiority of PSMA PET/CT over conventional imaging in the evaluation of the N- and M- staging (*7-9,31-34*), but its added value in the definition of T-staging and intraprostatic tumor localization is still controversial. The goal of our analysis was to compare the two imaging modalities in the definition of local disease and to evaluate if the combination of the two provides any significant advantage. In this setting the current literature shows discordant results, mostly due to small cohorts, different study designs and approaches in defining the imaging/pathology correlation. Differently from previous studies, in the current work we included a relatively large cohort of prospectively selected patients, and involved a standardized approach to image and whole mount pathology correlation analysis. An additional analysis on the T-staging was conducted, as well as a sub-analysis on lesions with lower Gleason grades (3+3=6). In our study, PSMA PET/CT allowed the detection of 4 lesions missed by mpMRI (4/109 lesions – 4%), but also misclassified more lesions as prostate cancer (higher number of false positives) at the expense of the PPV. An additional analysis specifically looking at negative lesions on both imaging modalities, discordant cases, and histopathological features of these tumor foci will be conducted separately by the authors in a future study.
The segment-level analysis for localization of prostate cancer foci did not show significant differences between PSMA PET/CT and mpMRI. Conversely, the addition of PSMA PET/CT to mpMRI significantly increased the number of segments detected, indicating that it improves the definition of tumor extent and can be an important aid in guiding the initial therapeutic approach (*5*). However, to confirm this finding further investigation is needed.

The results described above were obtained using a “neighboring” approach to evaluate imaging/pathology correlation, used to overcome the initrinsic limitation of the lack of registration between imaging and pathology. The use of PSMA PET/CT+mpMRI allowed the detection of 99% primary lesions and 69% secondary lesions, with an

overall detection rate of 87% (vs 85% and 83% for PSMA PET/CT and mpMRI alone, respectively) for all lesions, and 95% (vs 92% for both PSMA PET/CT and mpMRI alone) in clinically significant lesions (see supplementary table 2). Based on the improved performance of the combined PSMA PET/CT and mpMRI information, we recommend that discordant cases in the clinical practice should be evaluated in consensus between the PET/CT and MRI readers or during multidisciplinary prostate cancer tumor board. A lesion detected on only one of the modality should be considered susupicious. Whenever possible, the PSMA PET/CT and mpMRI images should be co-registered using the the CT and MRI prostate contours as reference.

mpMRI performed significantly better than PSMA PET/CT in the definition of the T-staging, i.e. SVI (T3b) and EPE (T3a), but not in the detection of bilateral disease (T2c). This finding is mainly attributable to the poor inter-reader agreement among the 3 PET readers for T-staging, probably due to the lack of standardized criteria for T-staging evaluation by PSMA PET/CT. On the contrary, since the correct definition of the locoregional extension of prostate cancer highly relies on anatomical detail visualization, the well-established higher soft tissue contrast, higher spatial resolution and multiplanar capability of mpMRI represent an advantage over CT and led to a good agreement between the 3 MRI readers for T-staging. However, inter-rater reliability was also poor for mpMRI readers in the evaluation of SVI. These results contrast with those of a previously published study involving 54 patients in which PSMA PET/CT showed higher sensitivity for the definition of EPE, but not for SVI (*35*).

Intra-prostatic tumor detection/localization by PSMA PET/CT relies largely on the PSMA PET signal because of the poor tissue contrast of CT. Consequently, lesion localization is highly dependent on the SUV visual scaling threshold used while interpreting the scans. Readers did not receive any specific recommendation on a fixed SUV threshold, as interpretation should be done by adapting the scaling to the background signal. This represents a source of inter-reader variability, but despite this inherent limitation for PSMA PET/CT, the segment-level analysis for localization of prostate cancer foci did not show significant differences compared to mpMRI.

Several studies showed that the combined use of PSMA PET/CT and mpMRI provides the best diagnostic accuracy overall (*10,14*). In light of the recent advent of PET/MRI, a growing body of literature is now available using PSMA PET/MRI, shown by several groups to outperform each modalitiy alone (*22,28,36-38*). However, the limited number of PET/MRI scanners available worldwide and the associated high costs still limit its widespread use in the clinical practice. The well-established superiority of PSMA PET/CT in the N- and M- staging, combined with an enhanced ability to determine T-stage and local extension with mpMRI, highlights the complementary role of each imaging modality and underscores the diagnostic potential of PSMA PET/MRI. If available, PSMA PET/MRI should be considered the modality of choice in the initial evaluation of patients with advanced prostate cancer. In case a hybrid PET/MRI scanner is not available, the PSMA PET/CT and mpMRI images acquired separately should be co-registered using a reproducible mutlilmodality DICOM image fusion tool. In case this is not possible, mpMRI remains the imaging modality of reference for the evaluation of the T-stage.

The main limitations of the study is the lack of co-registration between PSMA PET/CT, mpMRI and pathology and the absence of the use of 3D custom mold (*39-41*). To compensate for this inaccurate imaging/pathology correlation

limitation we used a “neighboring” approach. Another limitation is the time interval between mpMRI and RP was not homogeneous, ranging between 3 and 288 days, rising the potential issue of inherent tumor changes with time. Additionally, sources of bias include the lack of negative controls in the cohort, as all imaging readers were aware of the presence of biopsy-proven high- to intermediate-risk prostate cancer, and patient selection as we cannot rule out the exclusion of patients with a positive mpMRI and a negative biopsy from the final cohort. Thus, the PPV should be interpreted with caution. Finally, since we only included patients with intermediate and high-risk disease, we were not able to address the clinical question whether or not PSMA PET/CT can bring a significant added value to mpMRI in the initial staging of a heterogeneous population of patients with prostate cancer, including patients with less aggressive disease.

5. Conclusion

In our study using the majority reads of three blinded independent readers for each modality, both PSMA PET/CT and mpMRI performed well in the detection and intra-prostatic localization of intermediate- to high-risk primary prostate cancer, while mpMRI had superior performance in the definition of the T-staging (T2c, T3). The combined use of PSMA PET/CT and mpMRI improved tumor extent delineation. Our findings highlight the complementarity of the two imaging modalities.

DISCLOSURE

Johannes Czernin is a board member of Sofie Biosciences and founder of Trethera Therapeutics.

Jeremie Calais reports prior consulting activities outside the submitted work for Advanced Accelerator Applications, Blue Earth Diagnostics, Curium Pharma, GE Healthcare, Janssen, POINT biopharma, Progenics, Radiomedix and Telix Pharmaceuticals. He is the recipiend of grants from the Prostate Cancer Foundation (2020 Young Investigator Award, 20YOUN05), the Sociecy of Nuclear Medicine and Molecular Imaging (2019 Molecular Imaging Research Grant for Junior Academic FAculty), the Philippe Foundation INC. (NY, USA) and the ARC Foundation (France) (International Mobility Award SAE20160604150).

No potential conflicts of interest relevant to this article exist for all other authors.

KEY POINTS

QUESTION:

How does PSMA PET/CT perform in the local evaluation of primary prostate cancer in comparison to mpMRI? Is there an additional value in the combined use of both PSMA PET/CT and MRI in comparison to mpMRI alone?

PERTINENT FINDINGS:

Our analysis compared the performance of PSMA PET/CT and mpMRI for the local staging in 74 patients with intermediate- to high-risk prostate cancer using 3 blinded independent central readers for each modality. The two imaging modalities showed similar accuracy in the detection and localization of intra-prostatic lesions, while mpMRI performed better in the definition of extraprostatic extension and seminal vesicle involvement. The combined use of the two (PSMA PET/CT+mpMRI) leads to better cancer localization, but did not significantly improve detection rates.

IMPLICATIONS FOR PATIENT CARE:

In this study, the addition of PSMA PET/CT to mpMRI did not significantly change the local staging of patients with intermediate- to high-risk prostate cancer.

REFERENCES

1. Siegel RL, Miller KD, Jemal A. Cancer statistics, 2020. *CA Cancer J Clin.* 2020;70:7-30.

2. Mottet N, Bellmunt J, Bolla M, et al. EAU-ESTRO-SIOG Guidelines on Prostate Cancer. Part 1: Screening, Diagnosis, and Local Treatment with Curative Intent. *Eur Urol.* 2017;71:618-629.

3. Sanda MG, Cadeddu JA, Kirkby E, et al. Clinically Localized Prostate Cancer: AUA/ASTRO/SUO Guideline. Part I: Risk Stratification, Shared Decision Making, and Care Options. *J Urol.* 2018;199:683-690.

4. Johnson DC, Raman SS, Mirak SA, et al. Detection of Individual Prostate Cancer Foci via Multiparametric Magnetic Resonance Imaging. *Eur Urol.* 2019;75:712-720.

5. Johnson DC, Yang JJ, Kwan L, et al. Do contemporary imaging and biopsy techniques reliably identify unilateral prostate cancer? Implications for hemiablation patient selection. *Cancer.* 2019;125:2955-2964.

6. Silver DA, Pellicer I, Fair WR, Heston WD, Cordon-Cardo C. Prostate-specific membrane antigen expression in normal and malignant human tissues. *Clin Cancer Res.* 1997;3:81-85.

7. Hofman MS, Lawrentschuk N, Francis RJ, et al. Prostate-specific membrane antigen PET-CT in patients with high-risk prostate cancer before curative-intent surgery or radiotherapy (proPSMA): a prospective, randomised, multicentre study. *Lancet.* 2020;395:1208-1216.

8. Hope TA, Goodman JZ, Allen IE, Calais J, Fendler WP, Carroll PR. Metaanalysis of (68)Ga-PSMA-11 PET Accuracy for the Detection of Prostate Cancer Validated by Histopathology. *J Nucl Med.* 2019;60:786-793.

9. Lenis AT, Pooli A, Lec PM, et al. Prostate-specific Membrane Antigen Positron Emission Tomography/Computed Tomography Compared with Conventional Imaging for Initial Staging of Treatment-naïve Intermediate- and High-risk Prostate Cancer: A Retrospective Single-center Study. *Eur Urol Oncol.* 2020.

10. Rhee H, Thomas P, Shepherd B, et al. Prostate Specific Membrane Antigen Positron Emission Tomography May Improve the Diagnostic Accuracy of Multiparametric Magnetic Resonance Imaging in Localized Prostate Cancer. *J Urol.* 2016;196:1261-1267.

11. Berger I, Annabattula C, Lewis J, et al. (68)Ga-PSMA PET/CT vs. mpMRI for locoregional prostate cancer staging: correlation with final histopathology. *Prostate Cancer Prostatic Dis.* 2018;21:204-211.

12. Donato P, Roberts MJ, Morton A, et al. Improved specificity with (68)Ga PSMA PET/CT to detect clinically significant lesions "invisible" on multiparametric MRI of the prostate: a single institution comparative analysis with radical prostatectomy histology. *Eur J Nucl Med Mol Imaging.* 2019;46:20-30.

13. Kalapara AA, Nzenza T, Pan HYC, et al. Detection and localisation of primary prostate cancer using (68) gallium prostate-specific membrane antigen positron emission tomography/computed tomography compared with multiparametric magnetic resonance imaging and radical prostatectomy specimen pathology. *BJU Int.* 2020;126:83-90.

14. Chen M, Zhang Q, Zhang C, et al. Combination of (68)Ga-PSMA PET/CT and Multiparametric MRI Improves the Detection of Clinically Significant Prostate Cancer: A Lesion-by-Lesion Analysis. *J Nucl Med.* 2019;60:944-949.

15. https://www.accessdata.fda.gov/drugsatfda_docs/label/2020/212642s000lbl.pdf.

16. Schaeffer E, Srinivas S, Antonarakis ES, et al. NCCN Guidelines Insights: Prostate Cancer, Version 1.2021. *J Natl Compr Canc Netw.* 2021;19:134-143.

17. Tan N, Lin WC, Khoshnoodi P, et al. In-Bore 3-T MR-guided Transrectal Targeted Prostate Biopsy: Prostate Imaging Reporting and Data System Version 2-based Diagnostic Performance for Detection of Prostate Cancer. *Radiology.* 2017;283:130-139.

18. Natarajan S, Marks LS, Margolis DJ, et al. Clinical application of a 3D ultrasound-guided prostate biopsy system. *Urol Oncol.* 2011;29:334-342.

19. Eder M, Schäfer M, Bauder-Wüst U, et al. 68Ga-complex lipophilicity and the targeting property of a urea-based PSMA inhibitor for PET imaging. *Bioconjug Chem.* 2012;23:688-697.

20. Halpern BS, Dahlbom M, Quon A, et al. Impact of patient weight and emission scan duration on PET/CT image quality and lesion detectability. *J Nucl Med.* 2004;45:797-801.

21. Rosset A, Spadola L, Ratib O. OsiriX: an open-source software for navigating in multidimensional DICOM images. *J Digit Imaging.* 2004;17:205-216.

22. Eiber M, Weirich G, Holzapfel K, et al. Simultaneous (68)Ga-PSMA HBED-CC PET/MRI Improves the Localization of Primary Prostate Cancer. *Eur Urol.* 2016;70:829-836.

23. Rowe SP, Pienta KJ, Pomper MG, Gorin MA. Proposal for a Structured Reporting System for Prostate-Specific Membrane Antigen-Targeted PET Imaging: PSMA-RADS Version 1.0. *J Nucl Med.* 2018;59:479-485.

24. Rowe SP, Pienta KJ, Pomper MG, Gorin MA. PSMA-RADS Version 1.0: A Step Towards Standardizing the Interpretation and Reporting of PSMA-targeted PET Imaging Studies. *Eur Urol.* 2018;73:485-487.

25. Turkbey B, Rosenkrantz AB, Haider MA, et al. Prostate Imaging Reporting and Data System Version 2.1: 2019 Update of Prostate Imaging Reporting and Data System Version 2. *Eur Urol.* 2019;76:340-351.

26. Paner GP, Stadler WM, Hansel DE, Montironi R, Lin DW, Amin MB. Updates in the Eighth Edition of the Tumor-Node-Metastasis Staging Classification for Urologic Cancers. *Eur Urol.* 2018;73:560-569.

27. Turkbey B, Pinto PA, Mani H, et al. Prostate cancer: value of multiparametric MR imaging at 3 T for detection--histopathologic correlation. *Radiology.* 2010;255:89-99.

28. Hicks RM, Simko JP, Westphalen AC, et al. Diagnostic Accuracy of (68)Ga-PSMA-11 PET/MRI Compared with Multiparametric MRI in the Detection of Prostate Cancer. *Radiology.* 2018;289:730-737.

29. Koo TK, Li MY. A Guideline of Selecting and Reporting Intraclass Correlation Coefficients for Reliability Research. *J Chiropr Med.* 2016;15:155-163.

30. Lam TBL, MacLennan S, Willemse PM, et al. EAU-EANM-ESTRO-ESUR-SIOG Prostate Cancer Guideline Panel Consensus Statements for Deferred Treatment with Curative Intent for Localised Prostate Cancer from an International Collaborative Study (DETECTIVE Study). *Eur Urol.* 2019;76:790-813.

31. Kim SJ, Lee SW, Ha HK. Diagnostic Performance of Radiolabeled Prostate-Specific Membrane Antigen Positron Emission Tomography/Computed Tomography for Primary Lymph Node Staging in Newly Diagnosed Intermediate to High-Risk Prostate Cancer Patients: A Systematic Review and Meta-Analysis. *Urol Int.* 2019;102:27-36.

32. Koschel S, Murphy DG, Hofman MS, Wong LM. The role of prostate-specific membrane antigen PET/computed tomography in primary staging of prostate cancer. *Curr Opin Urol.* 2019;29:569-577.

33. Perera M, Papa N, Roberts M, et al. Gallium-68 Prostate-specific Membrane Antigen Positron Emission Tomography in Advanced Prostate Cancer-Updated Diagnostic Utility, Sensitivity, Specificity, and Distribution of Prostate-specific Membrane Antigen-avid Lesions: A Systematic Review and Meta-analysis. *Eur Urol.* 2020;77:403-417.

34. Zacho HD, Nielsen JB, Haberkorn U, Stenholt L, Petersen LJ. (68) Ga-PSMA PET/CT for the detection of bone metastases in prostate cancer: a systematic review of the published literature. *Clin Physiol Funct Imaging.* 2017.

35. Chen M, Zhang Q, Zhang C, et al. Comparison of (68)Ga-prostate-specific membrane antigen (PSMA) positron emission tomography/computed tomography (PET/CT) and multi-parametric magnetic resonance imaging (MRI) in the evaluation of tumor extension of primary prostate cancer. *Transl Androl Urol.* 2020;9:382-390.

36. Grubmüller B, Baltzer P, Hartenbach S, et al. PSMA Ligand PET/MRI for Primary Prostate Cancer: Staging Performance and Clinical Impact. *Clin Cancer Res.* 2018;24:6300-6307.

37. Muehlematter UJ, Burger IA, Becker AS, et al. Diagnostic Accuracy of Multiparametric MRI versus (68)Ga-PSMA-11 PET/MRI for Extracapsular Extension and Seminal Vesicle Invasion in Patients with Prostate Cancer. *Radiology.* 2019;293:350-358.

38. Thalgott M, Düwel C, Rauscher I, et al. One-Stop-Shop Whole-Body (68)Ga-PSMA-11 PET/MRI Compared with Clinical Nomograms for Preoperative T and N Staging of High-Risk Prostate Cancer. *J Nucl Med.* 2018;59:1850-1856.

39. Priester A, Natarajan S, Khoshnoodi P, et al. Magnetic Resonance Imaging Underestimation of Prostate Cancer Geometry: Use of Patient Specific Molds to Correlate Images with Whole Mount Pathology. *J Urol.* 2017;197:320-326.

40. Priester A, Wu H, Khoshnoodi P, et al. Registration Accuracy of Patient-Specific, Three-Dimensional-Printed Prostate Molds for Correlating Pathology With Magnetic Resonance Imaging. *IEEE Trans Biomed Eng.* 2019;66:14-22.

41. Wu HH, Priester A, Khoshnoodi P, et al. A system using patient-specific 3D-printed molds to spatially align in vivo MRI with ex vivo MRI and whole-mount histopathology for prostate cancer research. *J Magn Reson Imaging.* 2019;49:270-279.

Figures and tables

Table 1 - Patient characteristics. IQR= Interquartile range; PSA= prostate-specific antigen; ISUP= International society of urological pathology.

No. of patients	74
Median Age, yr (IQR)	65 (60 – 69)
Median PSA, ng/mL (IQR)	11.1 (7.5 – 21.5)
Initial PSA, ng/mL (%) ○ <10 ○ 10 – 20 ○ >20	 ○ 29 (39) ○ 26 (35) ○ 19 (26)
D'Amico Risk Classification (%) ○ Intermediate risk ○ High risk	 ○ 14 (19) ○ 60 (81)
Pre-surgical Gleason Grade (%) ○ 3+3=6 ○ 3+4=7 ○ 3+5=8 ○ 4+3=7 ○ 4+4=8 ○ 4+5=9 ○ 5+4=9	 ○ 1 (1) ○ 14 (20) ○ 2 (2) ○ 13 (19) ○ 24 (34) ○ 19(27) ○ 1 (1)

Table 2: Prostate cancer detection rates (lesion-based analysis)

Prostate cancer detection rates on a lesion-level of PSMA PET/CT, mpMRI, PSMA PET/CT+mpMRI (majority reads 2:1). Clinically significant lesions exclude lesions with Gleason score 3+3=6. Differences in detection rate between PSMA PET/CT and mpMRI were not statistically significant.

PPV= positive predictive value

	All lesions			Clinically significant lesions		
All Lesions	**PSMA PET/CT**	**mpMRI**	**PSMA PET/CT + mpMRI**	**PSMA PET/CT**	**mpMRI**	**PSMA PET/CT + mpMRI**
Index lesion (n=74)	72 (97%)	72 (97%)	73 (99%)	72 (97%)	72 (97%)	73 (99%)
Secondary lesion (n=32)	21 (66%)	19 (59%)	22 (69%)	18 (81%)	18 (81%)	19 (86%)
Tertiary lesion (n=3)	0 (0%)	0 (0%)	0 (0%)	0 (0%)	0 (0%)	0 (0%)
Overall (Detection rate)	93 (85%)	91 (83%)	95 (87%)	90 (93%)	90 (93%)	92 (95%)
PPV	97%	100%	-	94%	100%	-

Figure 1: Prostate segmentation template and imaging/pathology correspondence for lesion-based analysis.

12-segments subdivision of the prostate gland used for the standardized reads (left). Examples of imaging/pathology correlation for the lesion-level analysis using a ”neighboring” approach. The orange arrows indicate adjacent/neighboring segments.

Example 1: 1 lesion described on pathology as involving segments MRP, 1 lesion identified by imaging as involving BRP. Imaging/pathology correlation: TP finding because BRP and MRP are neighboring segments.

Example 2. 1 large lesion described on pathology as involving segments ARP, MRP, BRP, ALP and MLP, 2 lesions identified by imaging: lesion 1 involving ARP, MRP (yellow segments) and lesion 2 involving ALP, MLP (green segments). Imaging pathology correlation: TP because one single lesion was described on pathology and correctly identified as cancer by imaging, even though described differently.

Example 3. 2 lesions described on pathology: lesion 1 involving ALP, MLP, BLP, ALA, MLA, ARP and MRP (pink lesion) lesion 2 involving MRA (red lesion); 1 large lesion described by imaging as involving segments ARP, MRP, MLP, BRP and MRA. Imaging/pathology correlation: two TP findings because two lesions were described on pathology, and both were described as cancer on imaging.

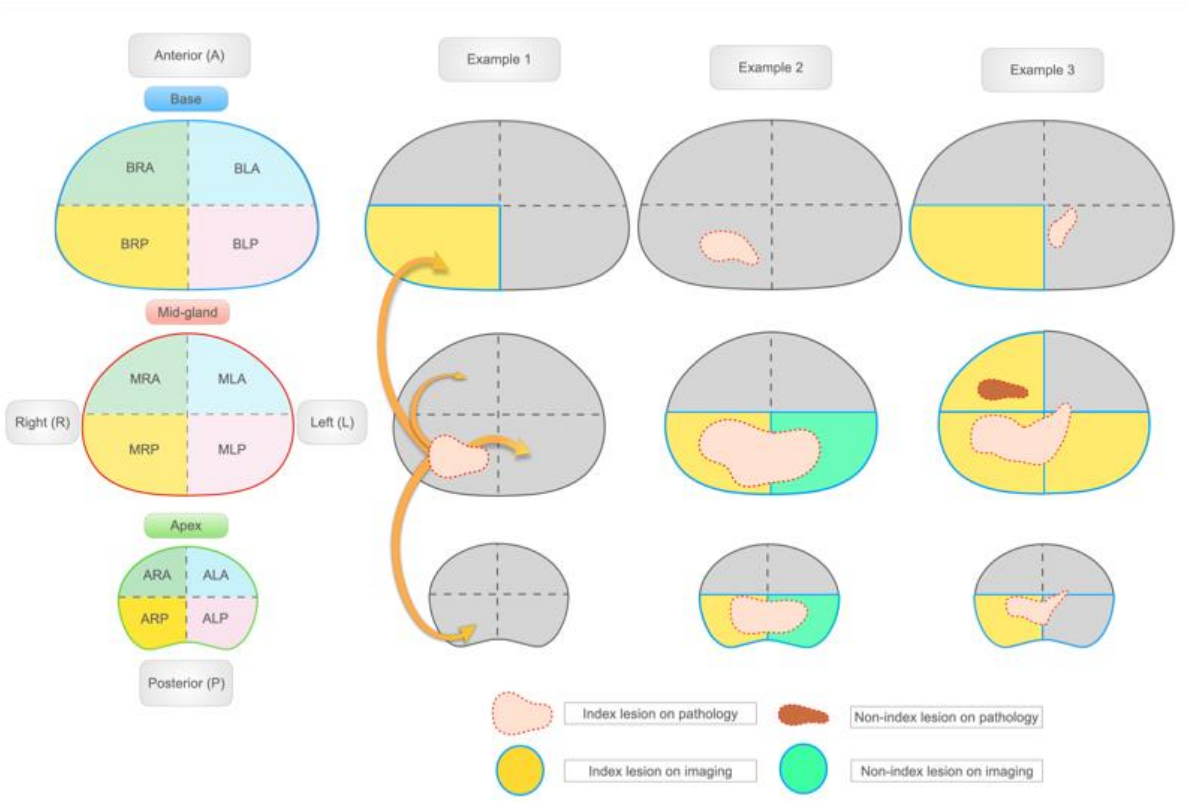

Figure 2: Study flowchart.

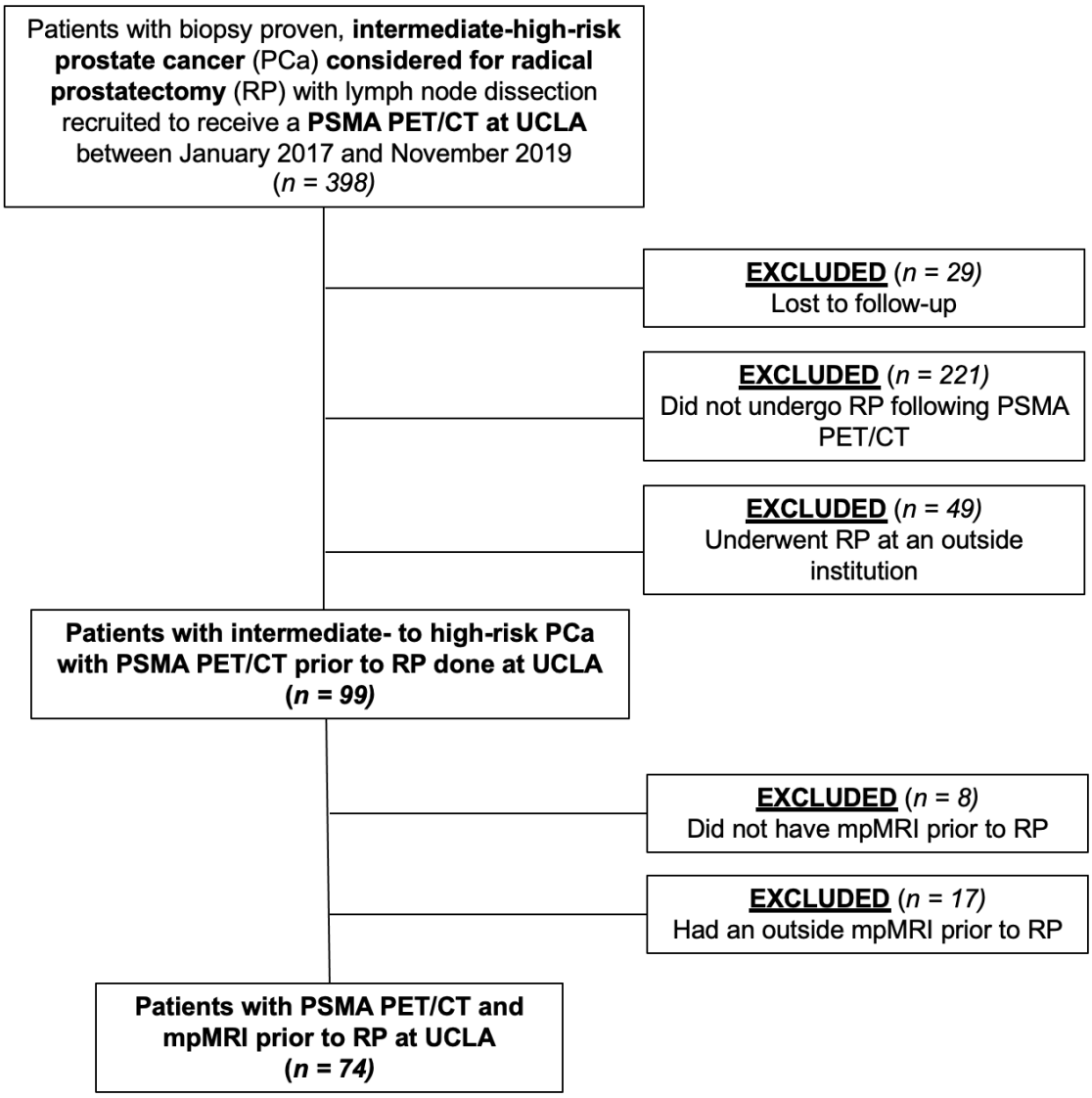

Figure 3: Prostate cancer localization (segment-based analysis) and T3-staging

Receiver operating characteristic (ROC) curves for the segment-level analysis obtained for the PSMA PET/CT and mpMRI majority reads (A), using the 1-to-5 PSMA and PI-RADS scores for each individual reader (B). ΔAUC between PSMA PET/CT and mpMRI (95% CI -0.01, 0.07; p= 0.093), PSMA PET/CT+mpMRI and PSMA PET/CT (95% CI 0.05, 0.1; p<0.001), PSMA PET/CT+mpMRI and mpMRI (95% CI 0.03, 0.06; p<0.001).

ROC curves for PSMA PET/CT and mpMRI majority reads in the evaluation of T-staging (C): bilaterality, extraprostatic extension and seminal vesicles involvement. ΔAUC for bilateral disease (0.65 vs 0.54 - DeLong's test p=0.138). ΔAUC for EPE (0.79 vs 0.59, 95% CI: 0.08-0.32; p=0.002) and SVI (0.84 vs 0.63, 95% CI 0.09-0.33; p=0.001).

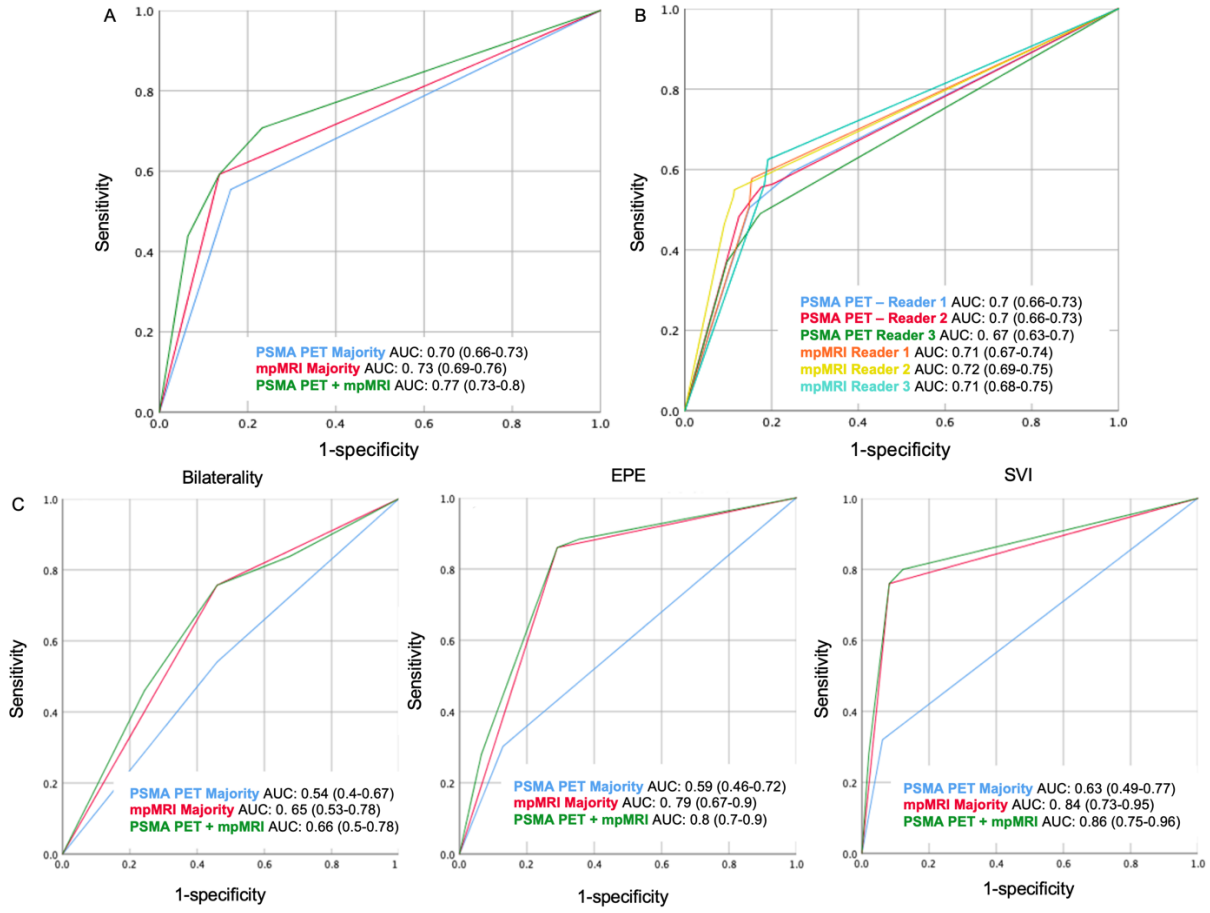

Figure 4: Two case examples from our cohort.

(Top row) 68-year-old patient (#4) with biopsy-proven prostate cancer Gleason score of 3+4=7 and PSA of 8.6 ng/ml at time of PSMA PET/CT. (A) Transverse PSMA PET/CT fused images, (B) T2-weighted and (C) high b-value diffusion-weighted (DWI) MR images show a right-posterior midgland lesion (green arrow). Whole mount pathology (D) shows one lesion, Gleason Score 4+3=7 in the same segment (contoured in green) and the lesion showed extraprostatic extension. Good imaging/pathology correspondence (true positive finding for both imaging modalities). All 6 readers correctly identified and described the lesion.

(Bottom row) 69-year-old patient (#5) with biopsy-proven prostate cancer Gleason Score of 3+4=7 and PSA of 11.4 ng/ml at time of PSMA PET/CT. Transverse PSMA PET/CT (E) shows two foci of increased PSMA uptake in the right-posterior (yellow arrow) and left-posterior apex (green arrow), respectively . PSMA reader 1 correctly described one lesion involving the left- and right-posterior apex, PSMA readers 2 and 3 described the left and right foci as 2 separate lesions. T2-weighted MR images (F) show an hypointense lesion and DWI (G) show diffusion restriction in the right- and left-posterior apex (green arrow). All MRI readers correctly described only one lesion. Whole mount pathology (H) shows one lesion encompassing both the right- and left-posterior apex (contoured in green) with extraprostatic extension. This is an example of the same lesion being described differently by PSMA PET/CT and whole mount pathology (true positive finding for both imaging modalities).

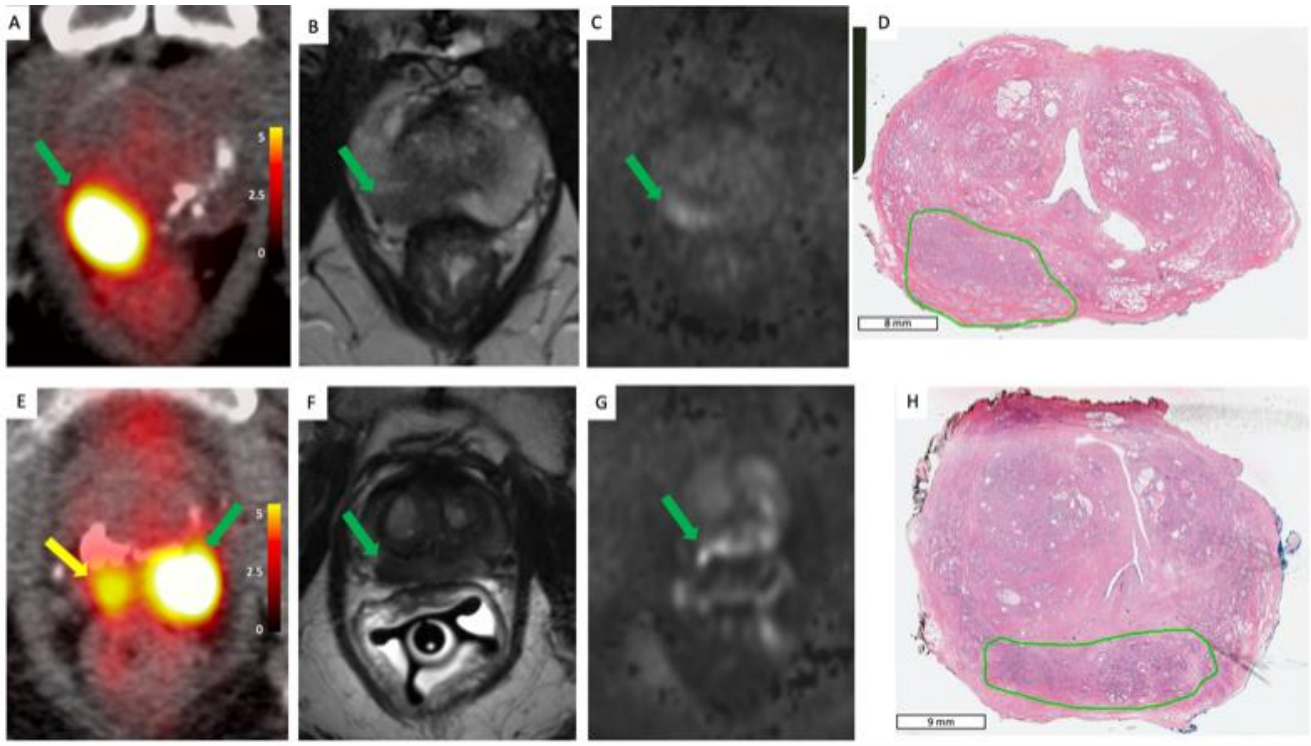

Graphical Abstract

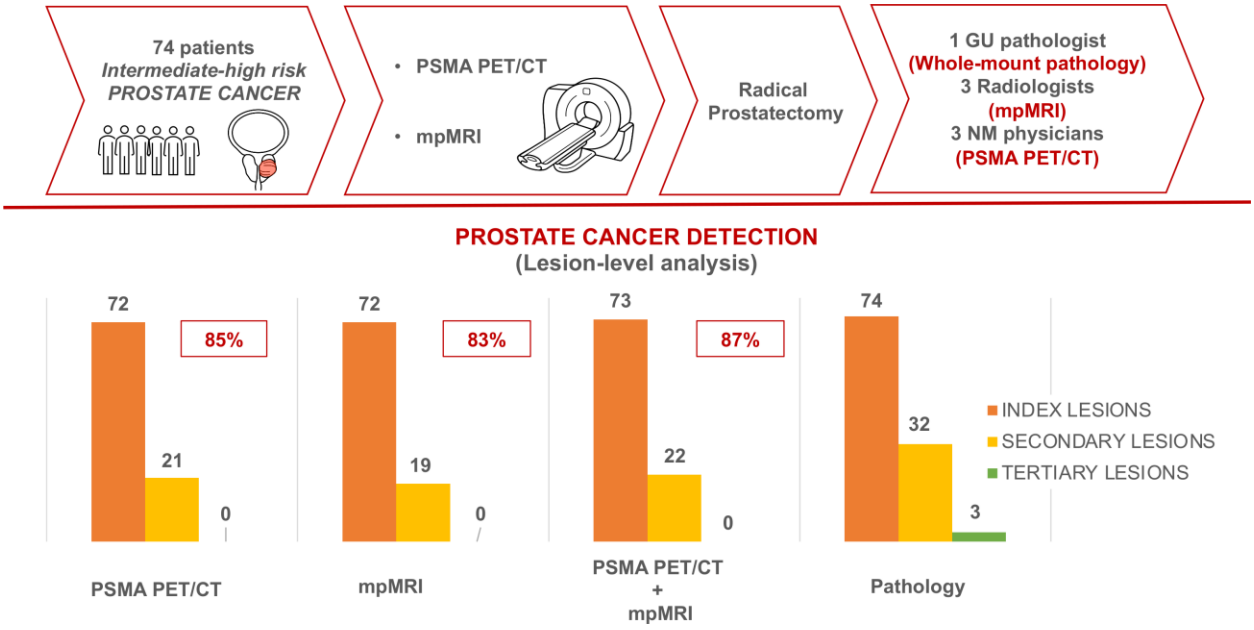

Supplementary Figures and Tables

Supplementary Figure 1: Receiver operating characteristic (ROC) curves for the segment-level analysis for clinically significant lesions (excluding Gleason score 3+3=6) obtained using a binary score for the PSMA PET/CT and mpMRI majority reads (left), using the 1-to-5 PSMA and PI-RADS scores for each individual reader (right).

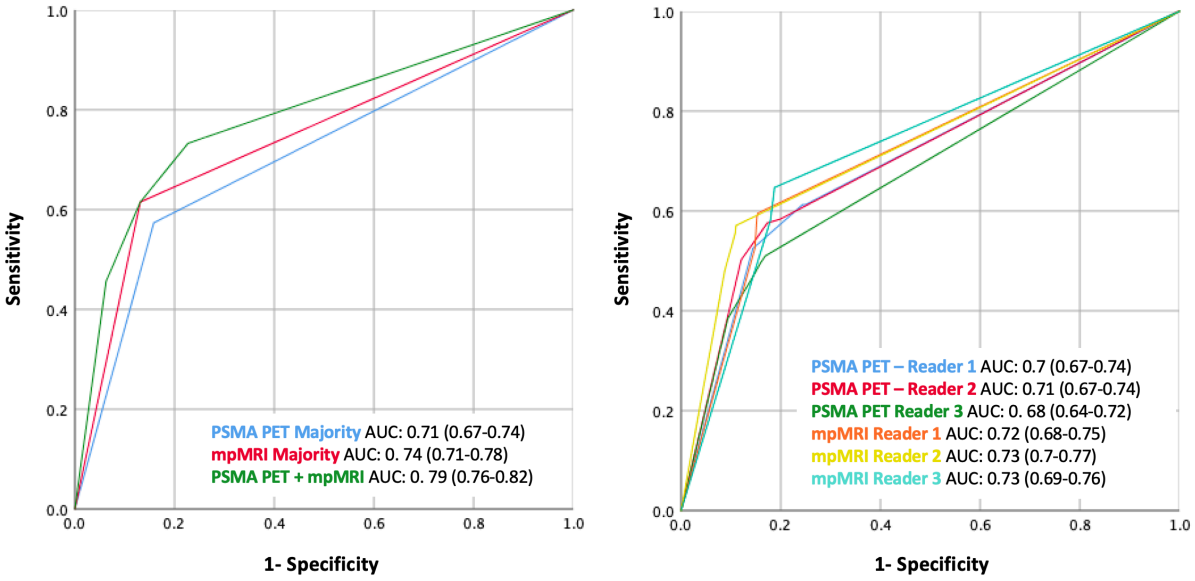

Supplementary Figure 2: Two case examples from our cohort.

(Top row) 61-year-old patient (#23) with biopsy-proven prostate cancer Gleason Score of 4+5=9 and PSA of 11.6 ng/ml at time of PSMA PET/CT. (A) Transverse PSMA PET/CT, (B) T2weighted MRI images show a large PSMA-avid and hypointense lesion, respectively encompassing the right-posterior/left-posterior (large yellow arrow) and right-anterior midgland (small yellow arrow). (C) high b-value diffusion-weighted (DWI) MR images show diffusion restriction in the same location. Whole mount pathology (D) shows two lesions located in the right-posterior/left-posterior midgland (Gleason Score 4+5=9 - contoured in yellow) and right-anterior midgland (Gleason Score 3+4=7 - contoured in green), respectively. This is an example of two lesions on pathology described as a single large lesion by both imaging modalities (two true positive findings – as yellow and green lesions were both described as positive for cancer by both imaging modalities).

(Bottom row) 68-year-old patient (#28) with biopsy-proven prostate cancer Gleason Score of 4+3=7 and PSA of 32.8 ng/ml at time of PSMA PET/CT. (E) Transverse PSMA PET/CT shows a lesion with intense PSMA uptake encompassing the left-anterior/left-posterior base (yellow arrow) and a smaller lesion with mild PSMA uptake located between the anterior- and posterior-right base (green arrow), T2weighted (F) and DWI MR images (G) show a hypointense lesion and diffusion restriction, respectively in the left-anterior base (yellow arrow). Whole mount pathology (H) shows two lesions respectively located in the left-anterior/left-posterior base (contoured in yellow) with Gleason Score 4+5=9, and in the right-anterior base (contoured in green) with Gleason Score 3+3=6. Despite mild PSMA uptake is visible in the right-anterior/posterior base lesion, only one of the three PSMA readers gave it a positive PSMA score and was therefore considered a false negative for both imaging modalities.

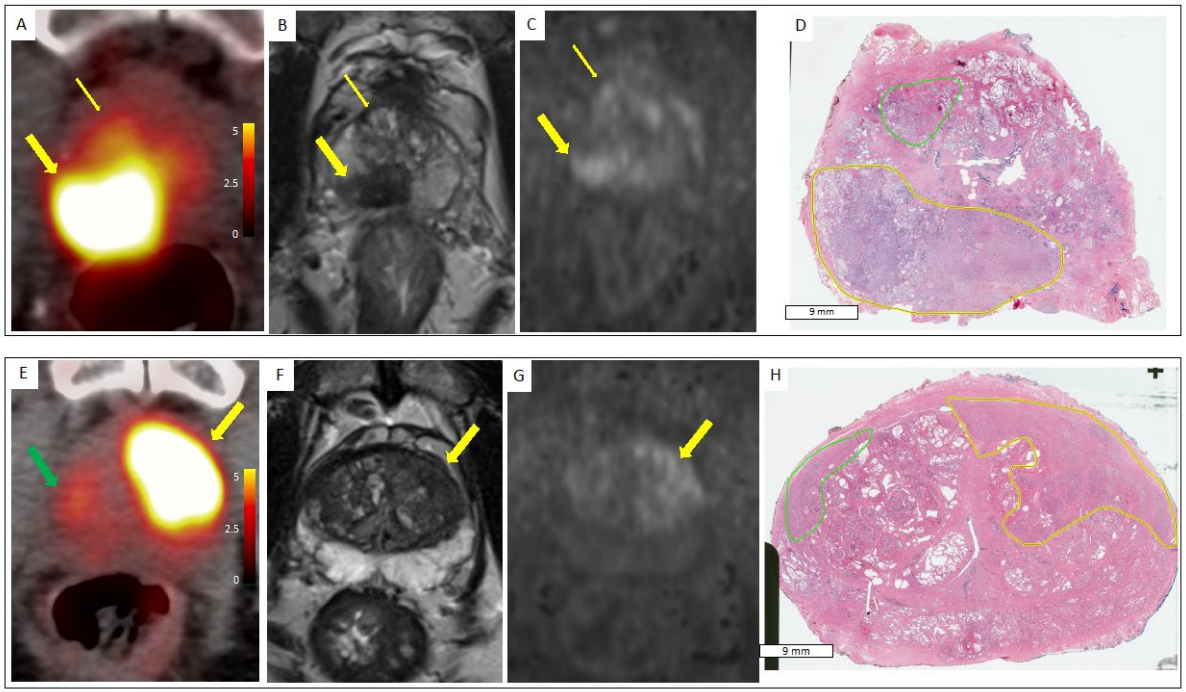

Supplementary Table 1: Prostate cancer detection on a lesion-level for each reader.
* McNemar test: p <0.05
PPV= positive predictive value

	PSMA PET/CT			MPMRI		
	Reader 1	**Reader 2**	**Reader 3**	**Reader 1**	**Reader 2**	**Reader 3**
INDEX LESIONS	74/74 (100%)	73/74 (99%)	73/74 (99%)	71/74 (96%)	72/74 (97%)	71/74 (96%)
SECONDARY LESIONS	20/32 (63%)	17/32 (53%)	17/32 (53%)	16/32 (50%)	19/32 (59%)	22/32 (69%)
TERTIARY LESIONS	0/3 (0%)	0/3 (0%)	0/3 (0%)	0/3 (0%)	0/3 (0%)	0/3 (0%)
OVERALL (SENSITIVITY)	**90/109 (83%)**	**94/109 (86%)**	**90/109 (83%)**	**87/109* (80%)**	**91/109 (83%)**	**94/109* (86%)**
PPV	97%	94%	92%	98%	95%	99%

Supplementary Table 2: Detailed performance of PSMA PET/CT and mpMRI in all lesions and clinically significant lesions.

All Lesions	PSMA+/MRI+	PSMA-/MRI-	PSMA+/MRI-	PSMA-/MRI+	Clinically Significant Lesions	PSMA+/MRI+	PSMA-/MRI-	PSMA+/MRI-	PSMA-/MRI+
Index lesions (n=74)	71 (96%)	1 (1%)	1 (1%)	1 (1%)	**Index lesions (n=74)**	71 (96%)	1 (1%)	1 (1%)	1 (1%)
Secondary lesions (n=32)	18 (56%)	10 (31%)	3 (9%)	1 (3%)	**Secondary lesions (n=22)**	17 (53%)	3 (9%)	1 (3%)	1 (3%)
Tertiary lesion (n=3)	0 (0%)	3 (100%)	0 (0%)	0 (0%)	**Tertiary lesion (n=1)**	0 (0%)	1 (100%)	0 (0%)	0 (0%)
Overall (n=109)	**89 (82%)**	**14 (13%)**	**4 (4%)**	**2 (2%)**	**Overall (n=97)**	**88 (81%)**	**5 (5%)**	**2 (2%)**	**2 (2%)**